Design of Supplementary Thrusting Unit for a Miniature Autonomous Submarine

William F. Newman

Thesis submitted to the faculty of the Virginia Polytechnic Institute and State University
in partial fulfillment of the requirements for the degree of:

Master of Science
In
Ocean Engineering

Wayne Neu
Craig Woolsey
Daniel Stilwell

November 19th, 2012
Blacksburg, Virginia

Keywords: Autonomous Underwater Vehicle, Secondary Propulsion Unit, AUV, SPU

Design of Supplementary Thrusting Unit for a Miniature Autonomous Submarine

William F. Newman

(ABSTRACT)

The focus of this work is to design and construct a version of the secondary propulsion units used on US Navy submarines for the Virginia Tech 690 autonomous underwater vehicle. These units were used to demonstrate a control system developed in a separate study which allowed the vehicle to autonomously perform advance maneuvers such as course-keeping, mooring and obstacle avoidance. The study of the miniaturized thrusters prompted an in-depth look into two thruster designs. The first was a retractable rim-driven propeller design which was found to be too power inefficient for implementation. The final design was an azimuthing ducted propeller capable of vectoring thrust 360 degrees. Two body sections containing an implementation of the ducted propeller design were constructed and mounted to the 690 vehicle. Tests were successfully conducted in a pool.

Acknowledgments

I would like to thank the entirety of the Autonomous Systems and Controls Lab at Virginia Tech for helping me the last 18 months. I would like to especially thank Dr. Wayne Neu, Dr. Dan Stilwell and Dr. Craig Woolsey for giving me this great opportunity and allowing me to work on such a unique project. I would like to thank Tim Pratt, Steven Portner, Brian McCarter and Aditya Gadre for lending me there time and expertise over the course of the project. Finally I would like to thank my family for supporting and believing in me over my entire college career and especially graduate school.

Contents

List of Figures

List of Tables

Chapter 1: Introduction

This paper describes the procedure followed in designing a secondary thrusting unit for implementation on an Autonomous Underwater Vehicle (AUV). The thruster was created as part of a larger project to design an Automated Submarine Propulsion-Enhanced Control (ASPEC) system for implementation on full scale submarines. The thrusters were implemented on a miniaturized submarine as a proof of concept for the ASPEC system.

Modern day U.S. Navy submarines are equipped with thrusters capable of providing an advanced level of maneuverability. Maneuvers such as mooring, mine avoidance or enemy interdiction are usually heavily dependent on the crew or possibly assistance from a tugboat. The ASPEC system was designed to autonomously perform complex maneuverers when the submarine is attempting to orient itself with respect to another body or local topography. With a proper control system these thrusters increase the independence of the vessel and the safety of the crew. When implemented the ASPEC system can reduce risk associated with human influence.

In addition to maneuvering scenarios SPUs provided advanced control in shallow water or harbor environments were the submarine must operate at low velocities. The maneuverability of underwater vehicles is often dependent on the speed of the water moving across their control surfaces. At high velocities displacing the control flaps produces a force that places a moment on the vehicle causing it to turn. At slower velocities the forces on the flaps are significantly decreased and the vehicle loses its ability to maneuver effectively. It is at these lower velocities that it becomes practical to implement a secondary thruster to restore maneuverability. In both these scenarios SPUs can be utilized to improve navigation with fewer crew and over time decrease the total cost of the vessel.

The AUV used to represent a scaled submarine in this study was the Virginia Tech 690. This is a general purpose ocean surveying vehicle designed by the Autonomous Systems and Controls Laboratory at Virginia Tech. The AUV, which can be seen in Figure 1, has an 80 inch long body with a maximum diameter of 6.9 inches. The 690 is depth rated for up to 500 meters and is capable of a cruising range of over 100 nautical miles. The body of the AUV is composed of four modular tube sections with a nose cone on the front and a tail section on the back. The sub's only means of propulsion and maneuverability is through its propeller and control flaps located on the tail section. In this study, two thrusters were to be implemented on the sub to increase its maneuverability enough to test the ASPEC system. One SPU was integrated behind the nose section and the other in front of the tail section.

The following sections follow the project as it works through the design process and ultimately converges on an azimuthing non-retractable SPU. The first half of the paper provides an in-depth analysis of a retractable rim driven thruster design. Due to high power consumption the idea was ultimately set aside. The second half of the paper discusses the design of the azimuthing concept by modification and augmentation of a purchased thruster. Finally the paper concludes by discussing the integration of the SPUs into the 690 AUV and plans for testing the maneuverability of the AUV.

Figure 1. Virginia Tech 690 AUV. The Virginia Tech 690 is a miniature submarine AUV designed for the purpose of conducting general purpose ocean surveying missions.

Chapter 2: Initial Concepts

2.1 Problem Statement

The goal of the SPUs was to design a thruster able to mimic the capabilities of an actuator that may be found on a commissioned Navy submarine. The most fundamental requirement of the design is that it should be capable of moving the submarine in the positive and negative sway and yaw degrees of freedom. In addition the thrusters must be able to operate effectively at low velocities. Though there is no set depth requirement for the thrusters the units must be water tight as any leakage could threaten the safety of the internal components of the submarine. In addition the deeper the thrusters are able to operate the more possible applications they could possibly have. The final requirement is that the entire unit must take up as little space as possible to limit the effect it has on the maneuverability of the vehicle.

Though not directly stated in the problem statement many other design constraints were set to allow easy integration into the 690 AUV. The foremost is that the thruster assembly must have a reasonable margin of positive buoyancy. This will allow for ballasting of the AUV and compensate for any additional electronics that are incorporated during the SPU integration. Another feature is that the thruster should be able to retract into the body of the sub. This cuts down on the overall drag of the vehicle when the thrusters are not in use. Retracting the thruster would also provide protection for the external components from collisions with external bodies. The final requirement, which is not dictated by the problem statement or integration into the AUV, is that the thruster be capable of azimuthing. This would greatly increase the maneuvering capabilities of the submarine.

2.2 Design Selection

Multiple thruster designs were studied and considered for implementation in the SPU. Two types of commercial thrusters were dissected to help better understand how miniature thrusters can be manufactured, assembled and sealed. Figure 2 shows the two types of thrusters that were dissected. Figure 2a shows a miniature Voith Schneider propeller. This type of propeller is usually mounted under a surface vessel. High aspect ratio blades protrude in a circular pattern from the face of the propeller. As the propeller turns, gearing at the base of the blades rotates the blades independently so that each blade is constantly producing positive thrust. The propeller is capable of producing thrust in any direction in the plane of the face of the propeller. The dissection of the thruster reviled many small parts that could be difficult to seal at high pressures.

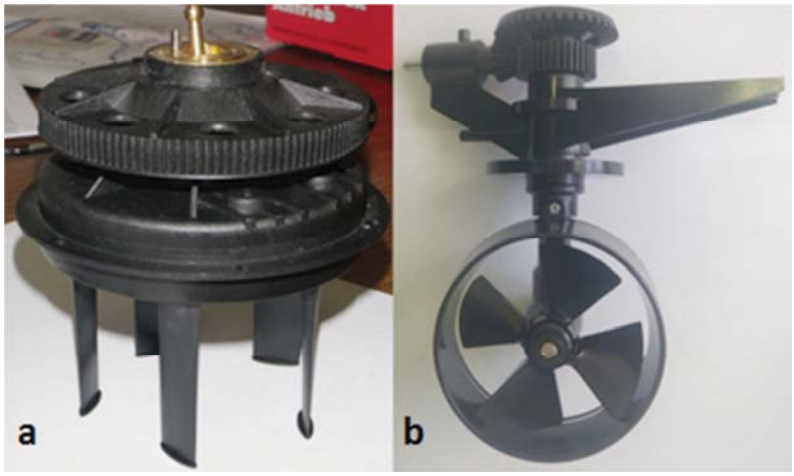

Figure 2. Purchased Thruster Designs. These two thrusters were dissected to get a better understanding of how a miniaturized thruster may be designed. (a) This is a Voight Schneider propeller. It can produce trust in any direction parallel to its face. (b) This is a Graupner Schottelantrieb II. This uses a traditional propeller.

The second thruster that was dissected was a Graupner Schottelantrieb II which can be seen in Figure 2b.This type of thruster also mounts to the bottom of a surface vessel but uses a traditional ducted propeller to produce thrust. In this design a hollow plastic 1.6 cm shaft penetrates the hull of the ship. The ducted propeller mounts to the back of a bullet shaped hub molded to the bottom of the hollow shaft. A network of metal gears and shafts inside the hollow shaft transfer the power from a motor mounted inside the hull of the ship to the ducted propeller. At the top of the unit, where the thruster mounts to the hull, the plastic outer shaft sits in a plastic bushing. A servo motor inside the hull of the ship rotates the outer shaft and directs the thrust. With minor modifications this thruster could be fit with shaft seals that would allow it to be completely submerged. [5]

2.3 Concept Creation

In the early design stage many concepts were considered. In order to obtain a solution that best met the requirements of the design no ideas were ruled out. Even if a thruster concept seemed farfetched it was still possible that it could be combined with other designs to create a feasible solution.

The first and most generic concept that was discussed was a fixed bow thruster. A bow thruster is a propeller that is often fitted into the hulls of large ships to help with docking and complex maneuvers. The thruster sits in a tunnel running through the bow of the ship facing in the sway direction. Implementing a thruster of this nature would only allow for thrust in the sway direction but would eliminate the need for the thruster to retract. Another benefit to this type of thruster is that it would eliminate any undesired torques on the sub due to drag or thrust. Figure 3 shows an example of how a bow thruster might be implemented in the submarine. Another option that was considered was a rotating bow thruster. In this design the tube holding the propeller would be capable of rotating in the roll direction and would be able to provide thrust in any direction other than forward and aft.

Figure 3. SPU Bow-Thruster Concept. This thruster design features a ducted propeller embedded in submarines hull. The location of the propeller eliminates any unwanted torques on the sub due to thrust or drag forces. The drawback is this type of thruster only provides thrust in the port and starboard directions.

Another design that was purposed was a non-retractable azimuthing shaft inspired by the Graupner Schottelantrieb II dissection. In this design a large hollow shaft would protrude from the body of the submarine. The bottom of the hollow shaft would be welded to a bullet-shaped gear housing. A drive shaft would run through the center of the large shaft and connect with a bevel gear in the gear housing. The propeller would be mounted on a small shaft that ran horizontally though the center of the gear housing. The shaft would be held in place by bushings fore and aft. A bevel gear in the middle of the shaft would transfer power from the main driveshaft to the propeller. This design could be easily sealed with the use of off-the-shelf rotary shaft seals. The downside to this design would be that it would increase the drag on the submarine and leave the propeller exposed to collide with elements in its environment. Figure 4 shows a drawing of this concept.

Figure 4. Non-Retractable Azimuthing Thruster Concept. This thruster would be easily sealed but would create additional drag when the sub was underway. Propeller is shrouded by a duct that is not shown.

The first design chosen for implementation was a retractable azimuthing rim driven propeller. Instead of having a hub in the center, the blades of a rim driven propeller are supported by a ring on the outside. This is advantages since the hub of the propeller and the adjoining lower

velocity blade sections can be removed. The propeller is powered by the drive shaft coming into direct contact with the outside ring. By moving the shaft connection point away from the props axis of rotation the torque required to drive the propeller is greatly decreased. Since the drive shaft is parallel to the face of the prop, this setup is very thin and consumes little space. When retracted the thruster would produce limited drag and be protected from collisions with external bodies.

Figure 5 shows the concept designed to implement the rim driven propeller. The design features a propeller carriage mounted bellow an electronics box in a flooded section of the sub. The box is suspended inside of the hull by a set of rails. Using these rails as guides the entire assembly will be able to move up and down allowing the propeller to deploy out of the bottom of the hull. In this drawing the thruster uses an acme lead screw with a bevel gear attached to the head to control its location inside of the sub. The electronics box located above the propeller is water tight and protects all electronics and actuators associated with the thruster. The electronics box will house two servos and one motor. One servo will turn the acne nut to deploy the propeller and the other will direct the carriage facilitating azimuthing thrust. The motor shaft will extend from the electronics box to turn the propeller. Dynamic seals mounted in the wall of the electronics box will prevent leaking around the shafts of the servos and motor. Below the electronics box sits the carriage that holds the propeller. The top of the carriage fits into a bearing that is set into the electronics box. This will allow the carriage to turn freely. A gear will be incorporated into the top of the carriage allowing it to mesh with the servo mentioned above. When the thruster is completely contracted the bottom of the carriage will be flush with the outside of the submarine eliminating any excess drag.

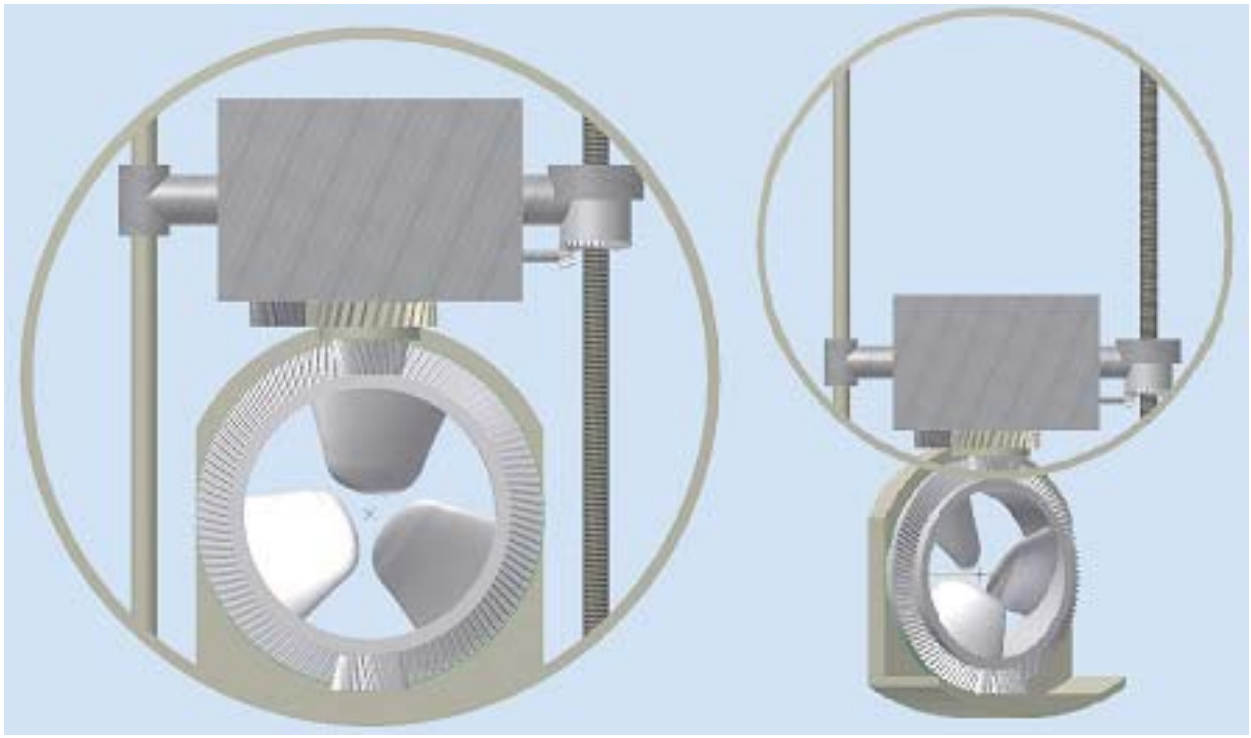

Figure 5. Rim Driven Thruster Concept. This image shows the first rendition of the rim driven thruster design.

Chapter 3: Rim-Driven Retractable Thruster Design

The rim driven propeller design was the first thruster studied for implementation in the submarine. The majority of the work done on this topic was put into designing an effective propeller. After studying many different aspects of the prop it was found not to be a feasible option. Ultimately the interactions between the outside ring of the propeller and the water created large energy losses. The following sections discuss all work completed to design the propeller and a customized rig used to test it.

3.1 Power Transfer

One of the first problems encountered with this design was effectively transferring motion from the driveshaft to the propeller. Initially the design called for a friction driven system where a rubber cylinder on the end of the driveshaft and textured surface on the propeller. Ideally the friction from the cylinder would transfer the rotation of the motor to the prop. Multiple tests were performed with different textures applied to the face of the prop. Fine textured faces performed well at low velocities but began to slip as the velocity was increased. Courser textured faces would hold contact for higher velocities but would cause irreversible damage to the rubber cylinder. It was concluded that a friction driven design was not a practical way drive the propeller.

In order to prevent slippage a gear was fitted to the face of the propeller. Two smaller gears of the same pitch where also designed. One was attached to the drive shaft to turn the prop while the other was implemented at the bottom of the prop to hold it in place.

3.2 Propeller Testing Platform

A custom rig was built to evaluate the performance of the propeller prototypes. The rig, shown in Figure 6a, was designed for measuring the thrust and power consumption of the propeller. The rig consisted of a board hinged on a stationary stand. Figure 6b shows the hardware mounted onto the board. A Hyperion motor at the top of the board was connected to a driveshaft that extended the length of the board to the propeller. The propeller was seated at the bottom of the board in a 70 mm bushing that was press fit into a metal frame. A stabilizing gear was mounted at the base of the frame to prevent the prop from slipping out of the bushing. This can be seen in the Figure 6c.

Once mounted on the stand the top of the board was connected to a force transducer. Any force produced by the propeller was felt by the board and measured by the transducer. Due to the moment arm associated with the hinged board the actual thrust was 59 percent of the force read off the transducer's display. During testing the stand was clamped to the side of a large tank of water. The prop was suspended well below the surface of the water to avoid bias due to surface effects. This set up can be seen in Figure 6a. It is important to note that since the propeller was fixed in the tank it experienced no forward velocity. Thus all flow across the blades was induced by the propeller. In actual applications this is often not the case since the momentum of the vessel often forces a flow across the propeller.

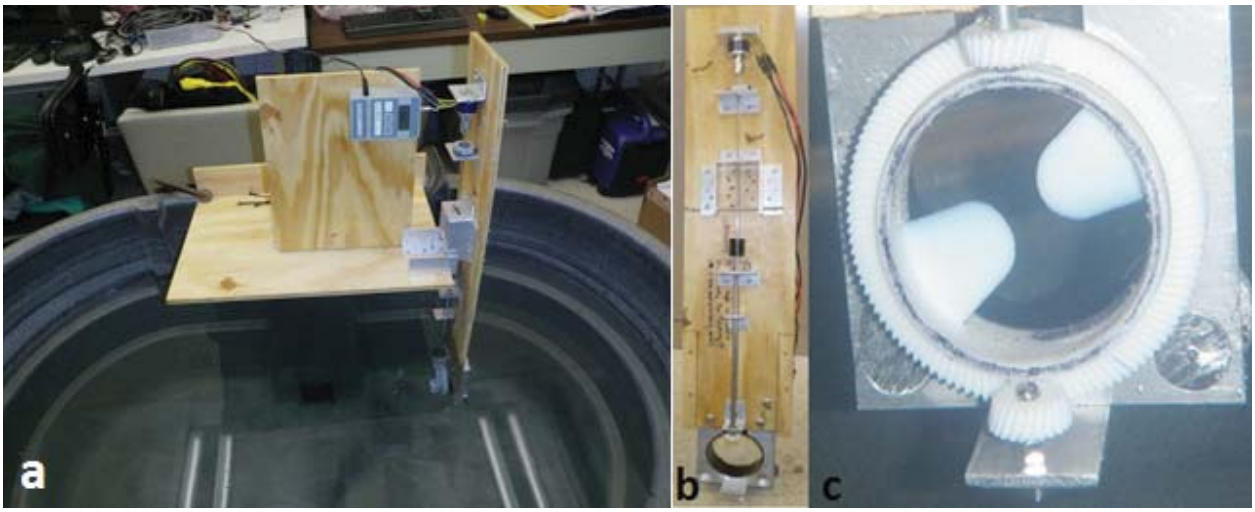

Figure 6. Propeller Testing Rig. (a) This picture shows the fully assembled test rig complete with a force transducer, hinge and mounting board. The rig is mounted in a tank of water that was used for testing. (b) This picture shows the mounting board. The top of the board holds the motor out of the water while the bottom holds the propeller. (c) This is the propeller mounted in its plastic bushing. The top gear is connected to the drive shaft while the lower gear holds the prop in place.

3.3 Blade Element Theory

Blade Element Theory (BET) was used for the initial design of the prop blades. This method was desirable due to its ease of use and short design time. This method treats the blade as a summation of a series of airfoil sections. Figure 7 shows an example of how a given airfoil section is evaluated.

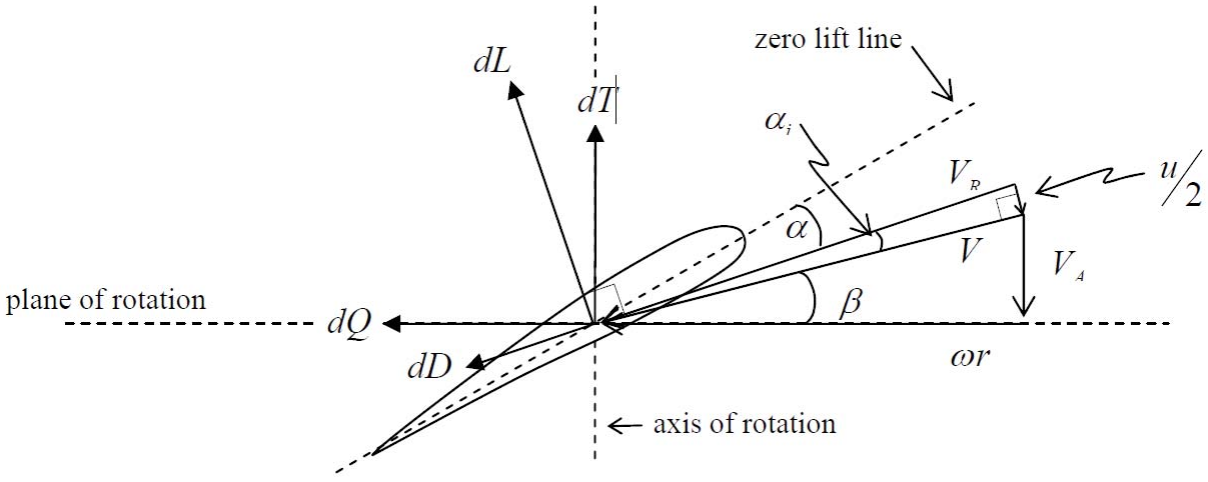

Figure 7. Blade Element Theory Airfoil Evaluation. This diagram shows all the forces and velocities taken into account when evaluating an airfoil section with blade element theory. [2]

Figure 7 shows the forces that are taken into account on an infinitesimally thick airfoil section. The fundamental forces the airfoil experiences are lift (*dL*), acting perpendicular to the blade's chord and drag (*dD*), acting along the length of the airfoil. Since the airfoil is a 2-D body

these quantities are measured in force per unit length. Equations 1 and 2 show the how the lift and drag forces on the airfoil are calculated.

$$dL = C_L * \frac{1}{2} * \rho * V_R * c \quad (1)$$

$$dD = C_D * \frac{1}{2} * \rho * V_R * c \quad (2)$$

In these equations C_L and C_D are the lift and drag coefficients that are functions of the airfoil's geometry and angle of attack. V_R, ρ, and c represent the overall velocity of the airfoil, the density of the fluid and the airfoil's chord length respectively[2, 3].

Since the lift and drag are determined with respect to the body of the airfoil they must be converted into quantities that can be directly related to the propeller. The two most convenient values are thrust (dT) and torque (dQ). The thrust is the force parallel to the axis of rotation. The torque is the resistance the propeller provides to rotation and is perpendicular to the axis of rotation. Both of these quantities can be seen in Figure 7. Equations 3 and 4 are used to rotate the lift and drag forces into the torque and thrust directions. Since dQ is a torque the entire equation is multiplied by a moment arm, *r*, the airfoils distance from the axis of rotation. In these equations α_i accounts for the downwash inherent in the three-dimensional blade. It is realized in the added flow velocity induced by the propeller. β is the angle that the incoming flow makes with the plane of rotation of the propeller. [2, 3]

$$dT_i = dLcos(\beta + \alpha_i) - dDsin(\beta + \alpha_i) \quad (3)$$

$$dQ_i = r[dLsin(\beta + \alpha_i) + dDcos(\beta + \alpha_i)] \quad (4)$$

Once the torque and thrust per unit length have been determined the total forces on the propeller can be found by integrating dT_i and dQ_i along the length of the blade. In practice it is much easier to treat the propeller as a series of constant cross-section airfoils with a finite width, dr. The forces on each section can then be calculated by multiplying the differential forces by the length of the section. The total torque and thrust on the propeller can then be found by summing the forces of the blade sections and multiplying by the number of blades, *Z*. [2, 3] This can be seen in Equations 5 and 6.

$$T = Z \sum_1^n dT_i * dr_i \quad (5)$$

$$Q = Z \sum_1^n dQ_i * dr_i \quad (6)$$

Though easy to use, blade element theory approximates the flow as two dimensional only traveling in the plane of the airfoil. As a result affects due to the flow along the length of the blade are not taken into account. These effects can often be neglected when designing long blades but could present problems when designing shorter blades such as on marine propellers. This theory also only acknowledges forces created by the propeller blades and therefore does not model the behavior of the propeller ring. This creates a large allowance for error when designing a propeller with a large ring on the outside.

3.4 Propeller Blade Design

In order to easily design and modify blade concepts BET was evaluated using an excel spreadsheet. A Clark-Y airfoil shape was chosen for the entire span of the blade. This is a generic airfoil shape that is common in older propellers due to its ease of manufacture. The spreadsheet used approximated the blade as a summation of ten finite airfoil sections. Inputs included RPM, forward velocity, number of blades and propeller radius, as well as, chord length and angle of attack at ten locations along the blade. Other values such as coefficients of drag and lift and blade thickness were determined by the characteristics of the Clark-Y shape.

The goal was to create a propeller that would operate over a wide range of velocities without experiencing stall. Stall is a phenomenon that occurs at high angles of attack when the flow on the backside of the blade separates, greatly reducing lift production. The difficulty in this is due to the fact that the angle of attack is affected by both the RPM of the propeller and the speed the fluid is moving orthogonal to the face of the propeller. As the RPM increases the angle of attach and lift on the blade increases inducing a flow perpendicular to the propeller. If the RPM is increased to quickly or the blades cannot induce an adequate flow the propeller will stall before an acceptable thrust is reached. The problem with this is that it is difficult to tell what the flow across the propeller will be without physical testing.

Once a blade design was completed Autodesk Inventor was used to draw the entire propeller. Two dimensional airfoil sections were lofted together to create the blades and a ring was extruded around the outside. Autodesk's gear design accelerator was used to create a geared surface on the prop and two small gears to be attached to a driveshaft and a stabilizing wheel on the bottom. The propeller models were manufactured with a 3-D printer. This type of manufacturing can be used to create complicated parts in a matter of hours with low cost. This type of manufacturing is only possible for small parts and often times the parts lack the durability due to the material with which they are printed. Since these propellers were only used for limited testing durability was not a major concern.

Numerous blade types and configurations were tested. The first propeller that was tested contained four evenly spaced blades with a low angle of attack. All blade segments had angles ranging from 10 to 15 degrees measured with respect to the face of the prop. The propeller was designed to run at speeds between 900 and 1700 RPM with a forward velocity of 3 f/s. In this range the prop was predicted to produce up to 2.9 lbs. of thrust.

During testing the propeller produced much lower thrust than predicted. Figure 8 shows the estimated Blade Element Theory (BET) thrust (green) and the measured thrust (red). At 1400 RPM the propeller failed to produce even a quarter of a pound of thrust. This is well below the thrust needed for the application of this thruster.

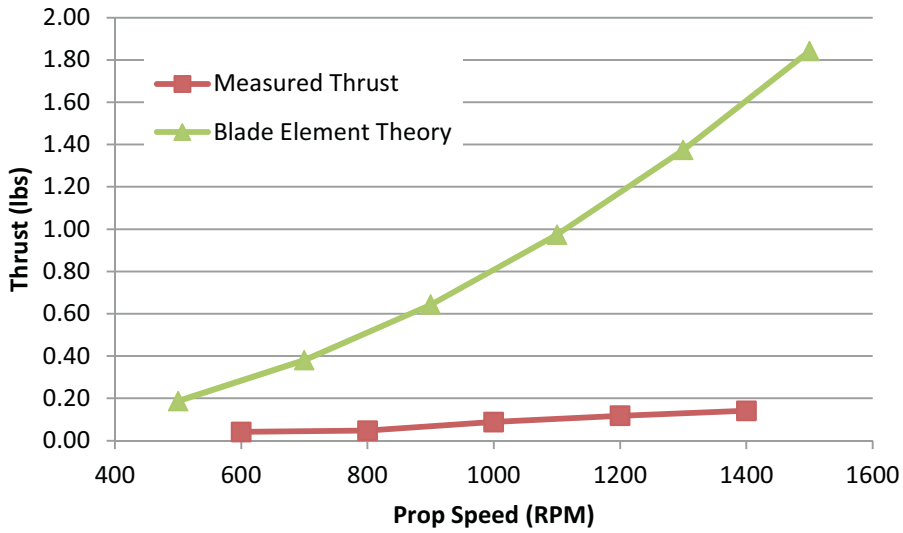

Figure 8. Actual and Theoretical Prop Thrust Production. The actual thrust produced by the prop was much lower than the theoretical thrust predicted by using blade element theory. This thrust is too low to effectively work with the thruster design.

One possible cause of the low performance of this propeller was the large number of blades in the prop. The large coverage provided by the blades left little space for the water passing through the propeller. It is possible that this caused the water to spin with the blades instead of passing through the prop. This hypothesis was tested by removing two of the blades from the ring. A file was used to remove one blade from either side of the propeller. This limited any eccentric loading on the prop.

Testing the altered prop showed only a slight increase in thrust. This was still well below the predicted values. This suggested that the prop's poor performance might be due to the design of the blades rather than covered area. This drew attention to many of the assumptions made during the design process, primarily forward velocity. While designing the blades the forward velocity of the propeller was assumed to be 3f/s. During testing the prop was fixed in a tub of water making its initial forward velocity zero. As the propeller began to produce thrust, water was pulled through the face of the propeller. Since this particular design produced little thrust and induced a smaller than estimated forward velocity, BET was unable to accurately predict its performance. Physically measuring the flow across the propeller and using this velocity with BET to recalculate thrust production would provide a much better model of the propeller. Since at this point it was clear that this propeller would not produce adequate thrust no further test was pursued.

3.5 Purchased Propeller Evaluation

After the failure of the initial prop design it was clear that the blades could not be properly designed without first knowing the induced forward velocity. Since there was no reliable way to determine this value it was decided to study the blades of a purchased propeller of similar size. Figure 9 shows the propeller that was studied to aid in the design of the rim driven prop. This propeller was taken from the dissected Graupner thruster. It contained four

blades and was powered by a shaft in its hub. The blades of this propeller had a constant angle of attack of 30 degrees which was much higher than the first rim driven design. The shape of the blades also appeared to be flat plates with chamfered edges. This suggested that the propeller might behave similarly in both the clockwise and counter clockwise direction. This propeller not only provided valuable insight on the blade design for propeller of similar size and RPM but also provided a benchmark for evaluating future renditions of the rim driven propellers.

Figure 9. Graupner Hub Driven Propeller. This prop was used as a basis for the design of the rim driven prop.

The Graupner propeller was tested by removing the metal frame from the bottom of the test rig and attaching the hollow plastic shaft of the Schottelantrieb II thruster. A wooden spacer was placed between the board and the plastic shaft to align the drive shaft of the Schottelantrieb II with the motorized shaft of the rig. It is important to note that the hub in front of the propeller altered the prop's inflow which may cause some discrepancies when compared with a rim driven prop with similar features. During testing both thrust production and power consumption of the rig were measured. Figure 10 show the thrust produced and power consumed by the propeller with increasing speed.

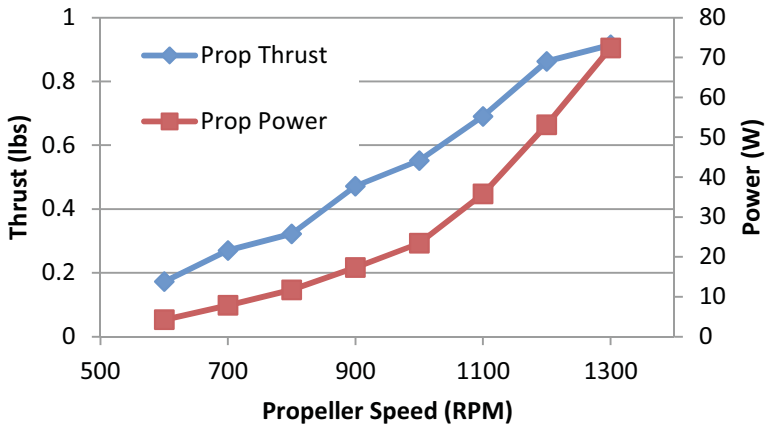

Figure 10. Thrust Production and Power Consumption of a Graupner Hub Driven Propeller. The Graupner propeller's performance acted as a benchmark for all future rim-driven propeller designs.

The thrust produced by the propeller appeared to vary nearly linearly with increasing RPM. At 1400 RPM the prop produced 1.14 lbs. of thrust. Given that ultimately two SPUs would be implemented, this was a considerable amount of thrust given that the main propeller of the 690 AUV produces 1.8 lbs. of thrust.

3.6 Rim Driven Propeller Redesign

Using data collected from the Graupner propeller two new rim driven propellers were designed. Despite the data from the examined propeller, forward velocity was still an important factor in the new designs. Given that the exact velocity was still unknown one propeller was designed to advance at 3 f/s and the other 6 f/s. Both designs contained three blades with a slight twist centered on a 30 degree offset from the face of the propeller. Since the 6 f/s propeller was assuming a faster advance speed it was also designed to operate in a slightly higher range of propeller speeds than the 3 f/s version. Figure 11 shows the two new propellers with the 3 f/s design on the left and the 6 f/s on the right. This figure also shows a chip in one of the blades of each propeller. This was due to the wear of the material over time and occurred during handling after the completion of testing.

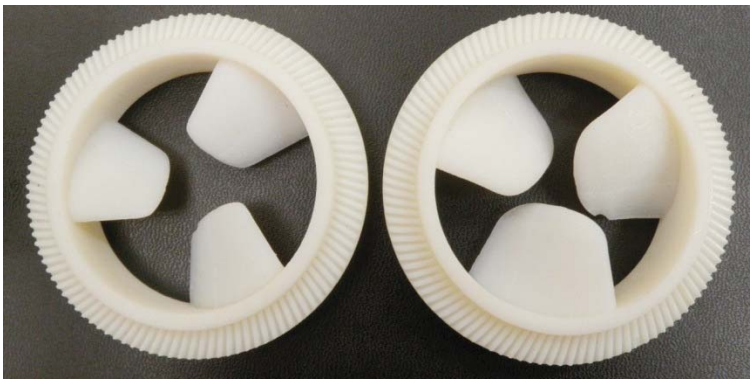

Figure 11. Large Blade Rim Driven Propeller Designs. These propellers are the 2nd and 3rd renditions of the blade driven design. The design for the blades of these propellers is based on the blades of a hub driven Graupner propeller.

Figure 12 shows the thrust produced by each propeller compared with the thrust measured from their purchased counterpart. The 3f/s version produced almost 0.09 lbs. of force more than the purchased propeller for every speed. The 6 f/s version produced the least thrust, lagging the purchased propeller by up to 0.178 lbs. at 1000 RPM. This suggested that for these propellers the induced advance speed in the tank was nearest to3 f/s.

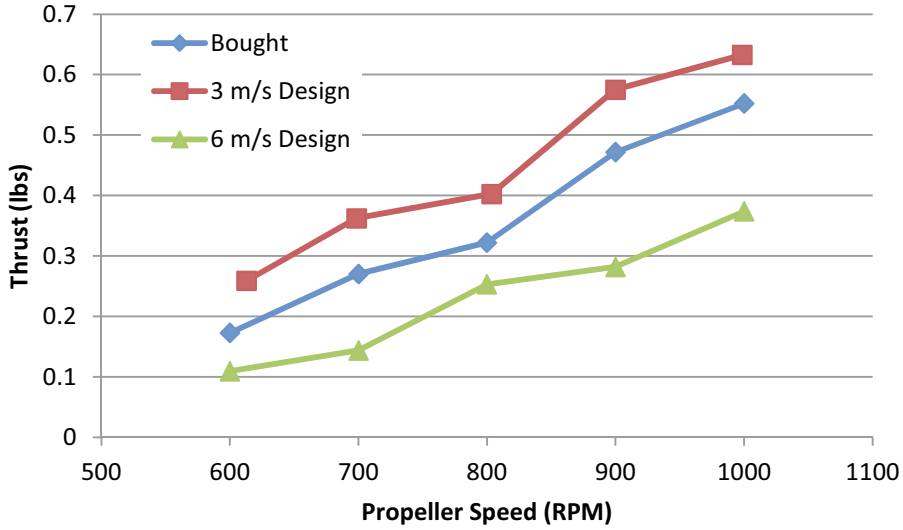

Figure 12. Thrust Production of 2nd and 3rd Generation Rim-Driven Propellers. At any given RPM the 3 f/s design produced 0.09 lbs. more thrust than the hub driven design. The 6 f/s design lagged the purchased prop by up to 0.178lbs.

Though the new designs produced thrust comparable to the purchased propeller their mechanical losses prevented the test rig motor form powering them above 1000 rmp. These losses are reflected in the power consumption of the propellers which can be seen in Figure 13. It is important to note that before each test the rig was run without the propeller to measure its mechanical losses. In Figure 13 these losses have been subtracted thus only showing the power consumption related to the propeller.

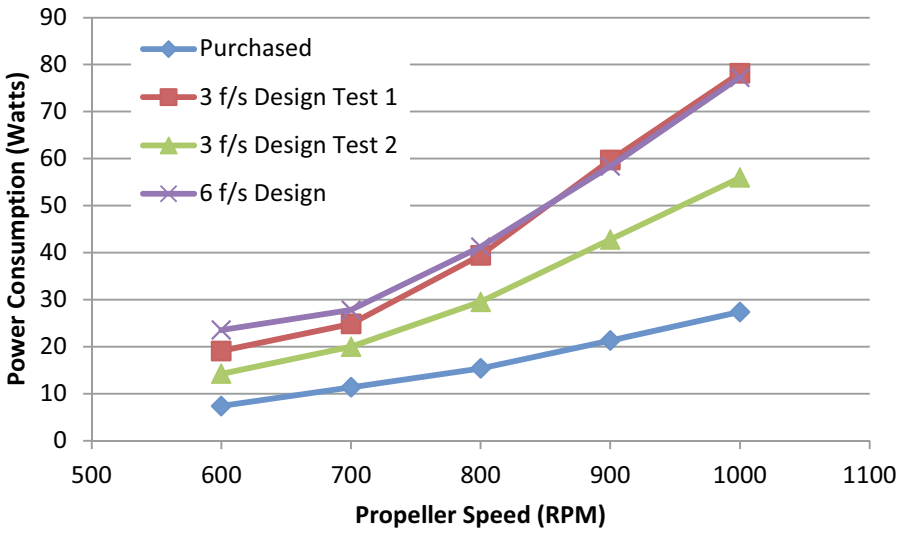

Figure 13. Propeller Power Consumption. All rim driven designs consumed considerably more power than the hub driven propeller.

In Figure 13 the bottom line represents purchased propeller and the top two lines represent the first tests of the 3 and 6 f/s models. At 600 RPM the rim driven designs consumed twice as much power as the traditional prop and the difference between the two increased with prop speed. It was hypothesized that the large losses were due to a clamping effect on the rim of the propeller between the bushing and the driving gear. To test this hypothesis a second test was run on the 3f/s model. In this test the prop was carefully adjusted so that the driving gear meshed with the prop without any additional clamping force. The results of this test are represented in the green (triangle) line in Figure 13.This new setup provided a 25% decrease in power consumption. Though this is notable decrease in power consumption it still represented a 50 percent increase over the traditional propeller design.

3.7 Gearing Hydrodynamic Analysis

With other factors eliminated the power consumption dilemma brought into question the hydrodynamic properties of the gears. During the original design the effects of the rotating gears on the water were assumed to be negligible due to their small size. Upon closer examination it was clear that the gears were stirring the water causing large power losses. As water was coming into contact with the rotating face of the gear it was accelerated outward and thrown tangentially away from the geared face. This was confirmed visually by a large static wave at the surface of the water above the rotating prop. Figure 14b shows the static wave formed on the left side of the plywood mounting panel.

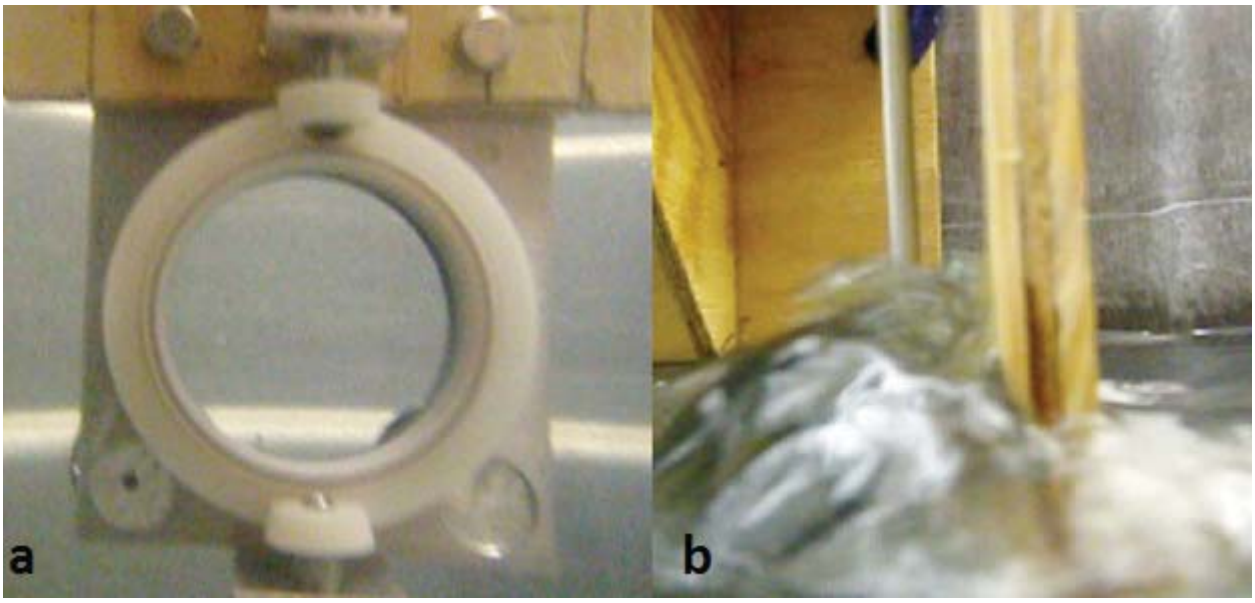

Figure 14. Water Disturbance Produced by a Geared Ring. (a) This bladeless ring was used to test the effects of the gears on the water.(b) The geared ring forms a large wave on the left side of the board while the water level on the right side remains undisturbed

To test the effects between the gearing and the water the final two blades were removed from the original rim driven prop. The bladeless prop is show in Figure 14a. Figure 15 compares the results of the geared ring test with second test on the 3 f/s design. The version without blades consumed nearly the same power as the version with blades as seen in Figure 15.

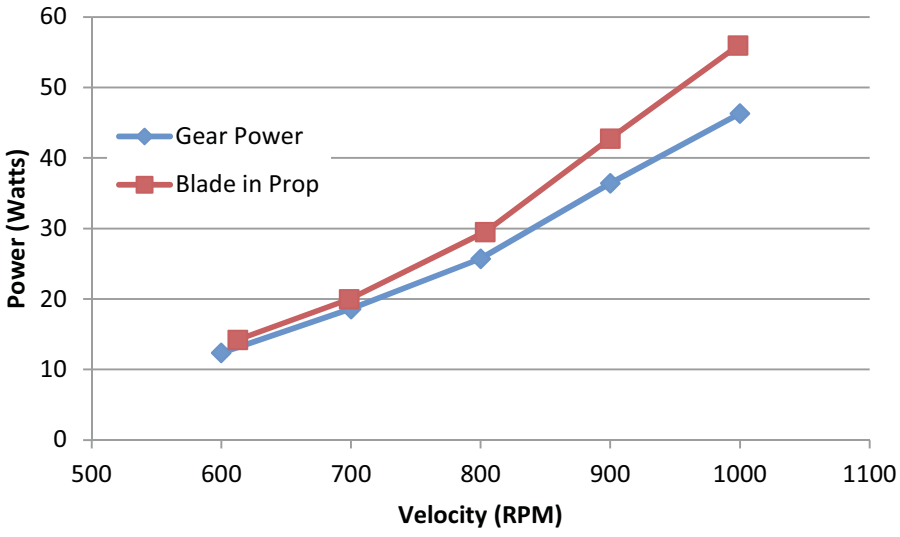

Figure 15. Geared Ring Power Consumption. The bladeless ring consumed nearly the same amount of power as the propeller with blades.

In an attempt to salvage the rim driven propeller concept two fairings were designed to minimize power loss. The first fairing was designed to reduce the flow around the gears. The design called for a thin covering that covered all geared surfaces of the thruster. This fairing can

be seen in Figure 16a. The idea behind this design was that the water trapped between the fairing and the geared face would rotate steadily with the gears and reduce power consumption.

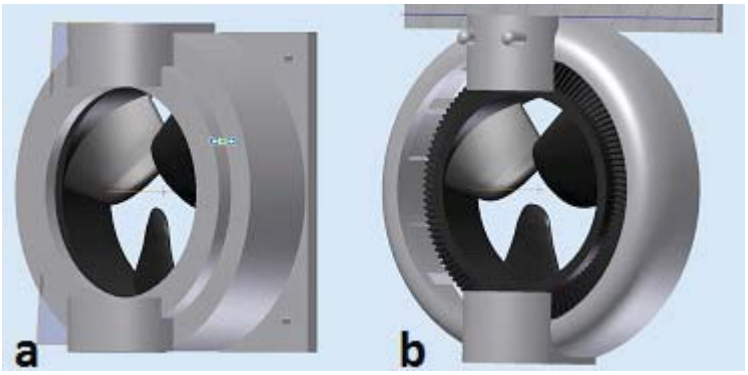

Figure 16. Fairing Concepts. (a) This fairing was designed to force the water to rotate steadily with the rotating gear. (b) This fairing was designed to redirect flow off the gears into thrust.

The second fairing was designed to harness the water being thrown from the face of the gears. This fairing can be seen in Figure 16b. A curved surface on the outside of the rim of the prop would capture the water and redirect it aft of the prop. This water would be providing additional thrust for the prop. The curved surface also contained veins to reduce the swirl in the flow. The driving and stabilizing gears in this design were covered in an attempt to reduce their effect on the flow.

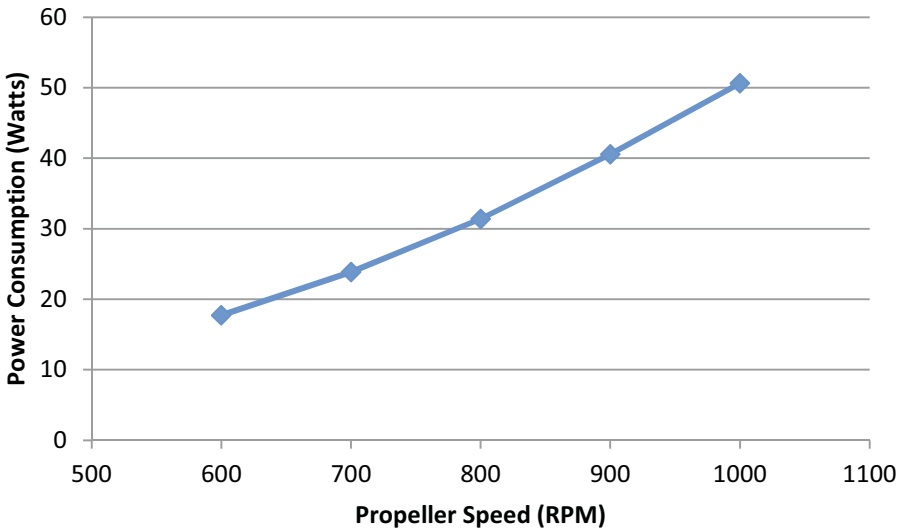

Figure 17. Covered Geared Ring Power Consumption. This figure shows the power required to operate the geared outer ring of the rim driven propeller when a cover has been implemented to muffle the flow.

Figure 17 shows the power consumption of the geared ring when implemented with the gearing cover. To prevent damaging the motor, data was only collected between speeds of 600 and 1000 RPM. The cover was found to increase the overall power consumption of the ring. The

close proximity of the cover to the face of the gears must have induced a shear in the water that greatly increased the torque on the propeller.

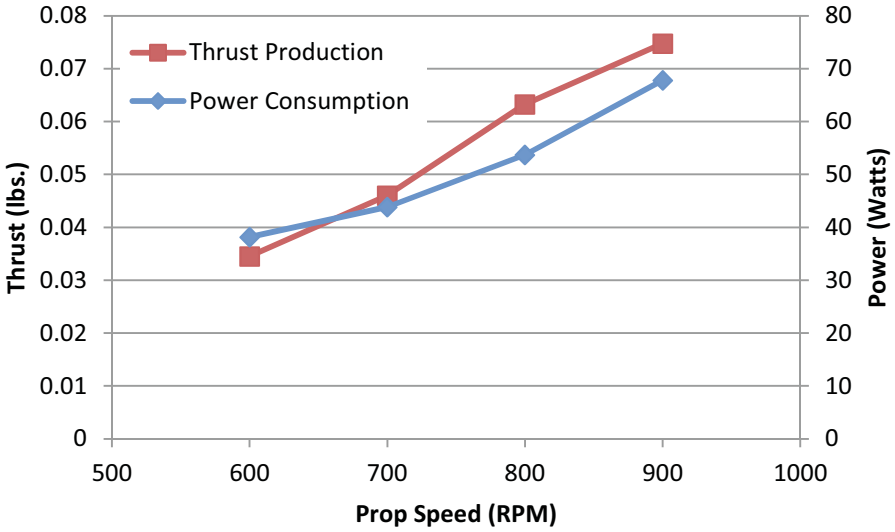

Figure 18. Flow Directing Fairing Characteristics. This chart shows the thrust and power consumed when a special designed fairing was implemented on the geared ring. The fairing captures the flow off the ring and redirects it as thrust. Ultimately the thrust production was not effective enough to compensate for the power losses.

Figure 18 shows the power and thrust consumption of the ring when implemented with the second fairing design. The amount of thrust produced by the fairing was minimal and did not adequately compensate for the power losses. Overall the fairings were found not to be a feasible way of increasing the efficiency of the propeller.

3.8 TSL Integrated Thrusters

While searching for ways to reduce power consumption on the rim driven propeller a product was discover that could greatly simplify the rim driven concept. TSL Technologies is a company based out of London, England that manufactures AUV thrusters and controllers. Their IntegratedThruster™ is a rim driven thruster with a motor integrated into the outside ring of the propeller. Figure 19b shows a cut away of the motor built into the outside ring of the propeller. Similar to the geared design, the blades sits inside a ring except instead of being geared this ring contains magnets. This effectively turns the entire propeller into a rotor. The outer ring, which acts as the stator, contains electro magnets that, when presented with an alternating current, turn the propeller. Figure 19a shows the IntegratedThruster™. [6]

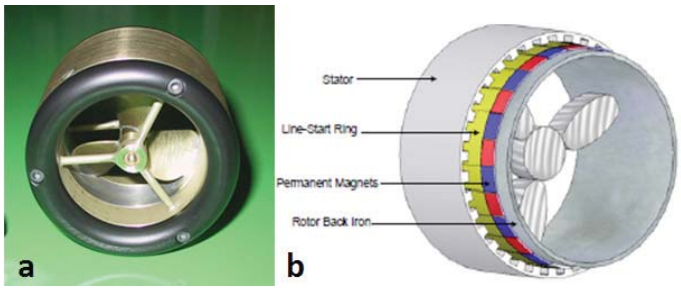

Figure 19. IntegratedThruster™.(a) This is the 50mm version of the IntegratedThruster™.(b) This cut away view depicts the inner workings of the thruster. [6]

This design resolves many of the current problems facing the SPU concept. Most notably this product has already been tested and shown to provide both sufficient thrust and efficiency when converting electric power to thrust. This design would also be much easier to seal due to the fact that all mechanical motions take place inside the ring of the propeller. From a sealing stand point this means that only electrical wires would need to protrude from the electronics box. When compared to the original design, which required a sealing surface on a rotating shaft, this is much simpler.

Due to limited time and funds on the project a new carriage was created to accommodate this thruster. This concept can be seen in Figure 20. Instead of occupying an entire tube section this design would be strapped to the underside of the sub. This design would be unable to retract but would also eliminate the need to manufacture a custom tube section to house the thruster. The electronics box, represented by the grey box in Figure 20, would mount directly to the sub's body. This box would hold a servo as well as a motor and servo controller. The IntegratedThruster™ would be mounted from a shaft suspended from the box. This shaft would be able to spin freely around its axis. A gear, mounted on the servo, would control the angle of the shaft giving the IntegratedThruster™ vectoring capabilities.

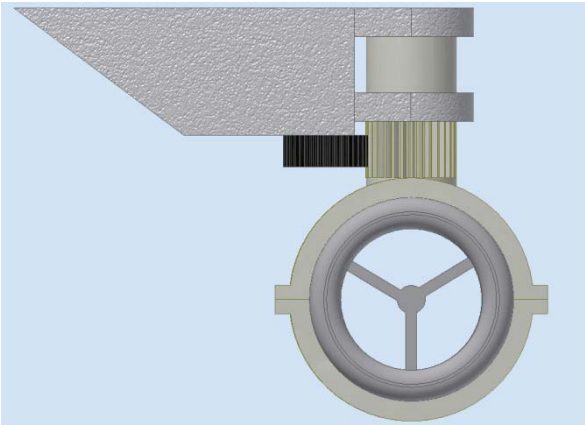

Figure 20. Fully External Thruster Concept. This concept was developed to implement the IntegratedThruster™. The thruster was designed to mount to the outside of the 690 AUV

After further examination into this thruster it was decided that it could not be implemented due to cost, time and physical constraints. The current submarine design does not contain an adequate number of ports to control machinery outside the hull of the sub. In addition

TSL Technologies quoted a cost of $3,000-4,500 per thrust and a turnaround time of two months. The potential of spending $9,000 was considered too costly for this aspect of the project and the associated extended turnaround time would leave inadequate time for assembly and proper testing.

3.9 Rim Driven Design Conclusions

A thruster design utilizing a rim driven propeller best fit the requirements laid down in the SPU project statement. The retractable carriage protects delicate components while the submarine is underway and reduces the drag associated with the thruster. The vectoring capabilities of the propeller would allow the submarine to perform complicated maneuvers at low speeds and in shallow water scenarios. The design could also be implemented in a relatively small tube section. However, an in-depth analysis of the rim driven design showed that this type of thruster could not effectively be implemented given the time, cost and physical constraints on the project. Perhaps if more time or funds were available a solution could be reached by utilizing IntegratedThruster™ or similar setup with minor design changes to the submarine. For the purposes of the SPU, however, with the project deadline approaching it was time to explore alternative thruster concepts.

Chapter 4: Non-retractable Azimuthing Thruster Design

4.1 Finalized Thruster Concept

After the rim driven concept had been thoroughly evaluated it was time to pursue alternative designs. As the project deadline approached time became one of the most important design criteria for the thruster. For this reason the non-retractable azimuthing thruster was investigated. This concept was inspired by the Graupner Schottelantrieb II which would provide a starting point for the new thruster design. As discussed earlier the Graupner Schottelantrieb II had been rigorously studied over the course of the project and though it was not the first alternative chosen, it displayed many desirable qualities. Earlier analysis revealed that the design could be easily sealed with minor modifications and the propeller was capable of producing adequate thrust. Perhaps more importantly the design could be quickly modified to fit into the submarine.

After a few weeks of extensive CAD design a final concept was ready for manufacturing. Figure 21 shows the final design which consisted of a ducted propeller mounted on a bullet shape gear hub. The hub was suspended below a small tube section by a ¾" aluminum shaft. Power was transferred to the propeller by two shafts and gears running through the hub and aluminum shaft. This hub and shaft combination was referred to as the lower housing. The lower housing was held in place by two bushings and a retaining ring inside of the tube section. This configuration allowed the housing to turn freely around the axis of the aluminum shaft. A duct mounted to the bottom of the housing propeller protected the prop and allowed for a larger thrust loading.

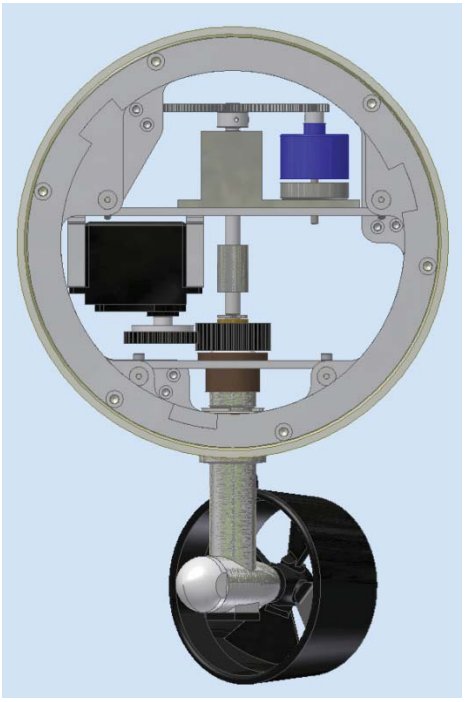

Figure 21. Final Non-Retractable Azimuthing Concept. This is the finalized SPU concept that was manufactured and implemented in the 690 AUV.

Inside the tube section two horizontal plates were used for mounting all internal components. The top plate held a motor and gearbox for running the prop and a servo for turning the lower housing. The bottom plat was embedded with a bushing that held the top of the aluminum shaft. The bottom plate was also wider than the top to allow the mounting of any electronics associated with the SPU. A second bushing was imbedded in the bottom of the tube section to align the aluminum shaft. A gear mounted at the top of the aluminum shaft provided an interface between the servo and the housing. Bulkheads fastened to either end of the tube section provided a mounting place for both plates.

4.2 Lower Housing

The component that was most heavily influenced by the Graupner Schottelantrieb II was the lower housing. The Graupner version and all major external features of the component can be seen in the left side of Figure 22. In the Graupner design the part is made from ABS plastic. Everything above the hull mount, extruded half way down the part, sits inside the hull of the ship and all features below are exposed to the water. The grooved portion above the hull mount fits into a plastic bushing fixed inside of the ship allowing it to turn freely. A gear mounted above the bushing allows for thrust vectoring. Below the hull mount the shaft exhibits a hydrofoil cross-section for reducing drag on the thruster. The bullet hub at the bottom of the part houses two gears for transferring power from a vertical driveshaft running down the length of the part and a horizontal shaft that runs through bullet hub. The head of the bullet screws off to allow for installation of internal components. Tapped holes below the hull mount and at the bottom of the bullet act as mounting locations for the duct.

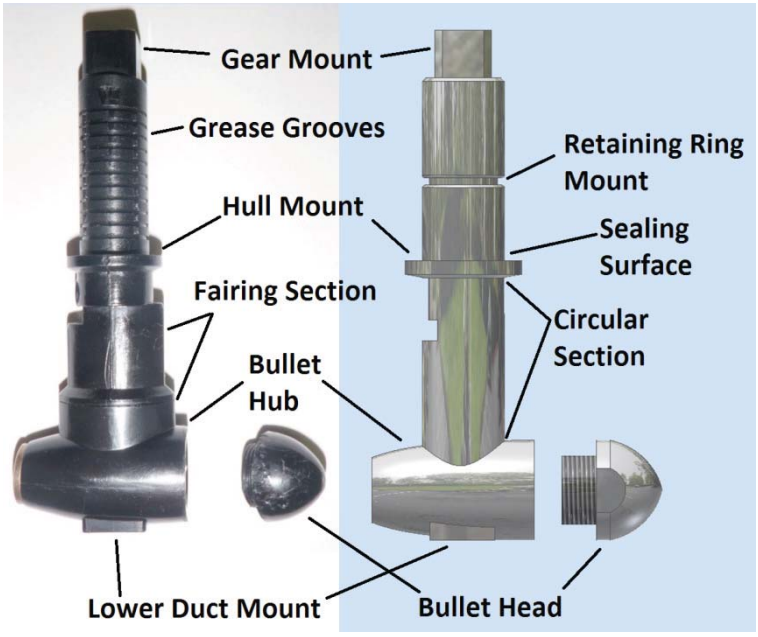

Figure 22. Graupner and SPU Lower Housings.(left) The Graupner lower housing was made of ABS plastic and had many features that prevented it from being implemented in the SPU.

The thruster is sealed by rubbing grease into the grooves at the top of the shaft. This sealing method is adequate for the low pressures experienced by surface ships but is not suitable for application on submersibles. For this reason a higher pressure rated seal needed to be

implemented on the shaft. PTFE spring loaded shaft seals are often used for these applications however the grooves in the shaft and the rough texture of the plastic prevented any usable sealing surfaces. Due to the number of modifications that would be needed to implement the Graupner housing, the decision was made to redesign the part and manufacture it out of 6061 aluminum.

The right side of Figure 22 shows the redesigned lower housing. In the redesign the vertical cylindrical portions of the housing were enlarged so that the shafts could be fitted with off the shelf seals. A 3/4 inch PTFE seal was fitted on the sealing surface directly above the hull mount. Just above the sealing surface a groove was cut into the shaft for mounting a retaining ring. The retaining ring was used to lock the housing in place once inserted into the tube section. In order to reduce manufacturing costs the fairing above the bullet was replaced with a circular cross section. The hub head was altered to include more threads to assist with sealing and two flats were machined on the sides so a wrench could be used for removal. To prevent any damage due to elements in the marine environment all features below the sealing surface were anodized.

Figure 23 shows the internal components of the redesigned lower housing. Letter A in the figure shows the main driveshaft running the length of the housing. The 1/4 inch shaft runs from the gear box to the bullet hub at the base of the housing. A bushing at the top of the housing and another just above the bullet represented by C and D hold the shaft in place. A secondary horizontal drive shaft represented by B, runs from the bullet head out the back of the bullet to the propeller. This shaft changes diameters along its length to allow for mounting of the gears and propeller. This driveshaft is also held in place by a bushing in the head and another behind the bullet. These are represented by E and F in the picture respectively. A bevel gear mounted on the end of both drive shafts transfers the power from the motor to the propeller.

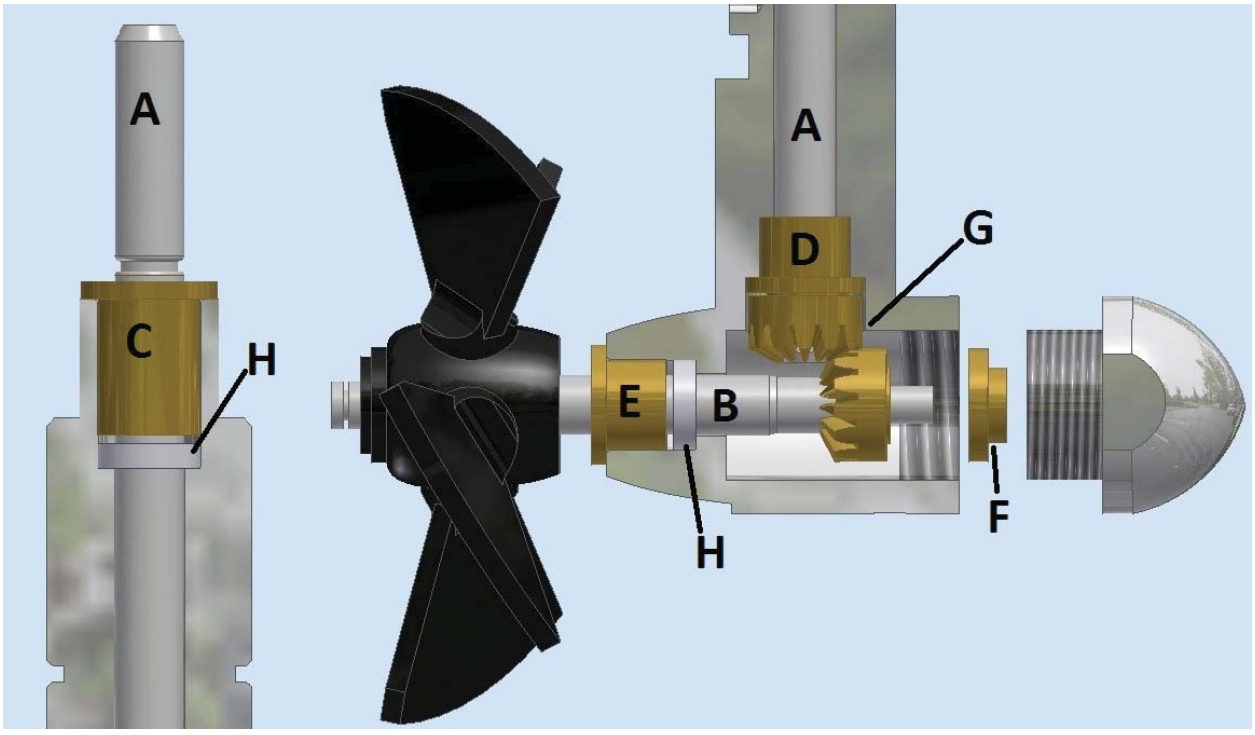

Figure 23. Lower Housing Internal Components. This figure shows a cut away of the lower housing revealing all internal components.

Three sealing surfaces were designed into the new lower housing. The inside of the bullet is sealed by a ¼" PTFE seal behind bushing E. The bullet head is also sealed by a combination of PTFE sealing tape on the threads and liquid gasket in-between the faces of the head and the bullet. A back up seal was also implemented below bushing C. This seal will prevent the AUV from flooding if either of the other seals is breached. Both PTFE seals are represented by H in Figure 23.

4.3 Tube Section

The tube section provides the structural base for all other components of the thruster. The structural design for the tube section itself is based off work done by the Autonomous Systems and Controls Lab at Virginia Tech in the development of a self-mooring AUV. The shell was machined out of 6061 aluminum and anodized to harden and protect the material. The outside diameter of the shelf is 6.9 inches to match the diameters of adjacent tube sections. Figure 24 shows a cut away of the SPU tube section.

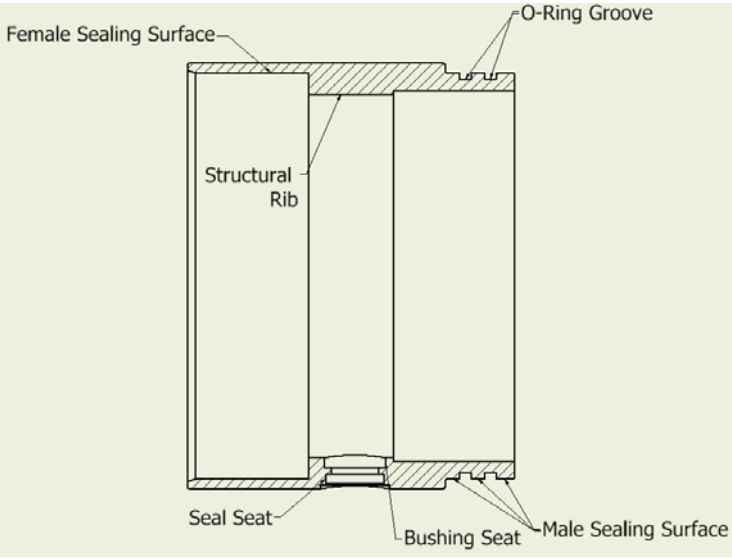

Figure 24. SPU Tube Section Cutaway View. The finalized tube section has four main features. Two end glands to allow interfacing with adjacent tube sections. A rib for structural support and a thruster port where the lower housing intersects the tube.

The tube section has four main features: A male gland, a female gland, the thruster port and the structural rib. The glands on either side of the tube allow for a high pressure seal to be formed with adjacent tube sections. The male gland is an indented portion shown on the right side of Figure 24. The indention allows the section to fit inside of the female gland of the adjoining tube section. The two groves on the surface hold O-rings to ensure a watertight seal. The female gland is comprised entirely of a smooth cylindrical surface. The surface holds the male interface of the adjoining sub section and forms a water tight seal with the O-rings. Once the AUV has been assembled a vacuum is pulled on the inside to ensure a firm connection between tube sections. The interfaces in the forward SPU are slightly longer than the aft to accommodate the connection with the forward sub sections.

The structural rib and thruster port allow the lower housing to protrude from shell section. Greater wall thickness in the rib ensures the tube section does not fail under pressure due to the thruster port hole. The thruster port has two main features. The inside of the port consists of a bushing seat that holds a ¾" Oilite bushing used to constrain the shaft and gear housing were it enters the tube section. The outer side of the port consists of a seal seat for the ¾" PTFE shaft seal on the outside of the gear housing. A flat section is milled into the outside of the tube section to allow an even resting spot for the gear housing hull mount.

The length of the tube section was dictated by the desired buoyancy of the SPUs. During the design process it was decided to make the SPU no less than 0.2 lbs. buoyant. This would allow for ballasting when the tube sections were integrated into the submarine. The buoyancy and weight of the tube section was evaluated by simplifying the tube section and using Autodesk Inventor to approximate the weight of the assembled tube section. The tube section, aluminum shaft and bullet were idealized as cylinders and all other features were assumed negligible. Only the female gland was included in the volume estimates since the male gland would be imbedded in another tube section. Autodesk inventor measured an overall weight of 5.5 lbs. for the assembled tube section. A net buoyancy force of 0.21 lbs. was achieved by creating a combined female gland and body length of 4.187 in.

4.4 Bulkheads

The bulkheads provide a means of interlocking adjacent tube sections, as well as, providing attachment points for the rails that hold the mounting plates in position. The SPU has three types of bulkheads. Figure 25 shows the male, female and mounting bulkheads positioned from left to right, respectively.

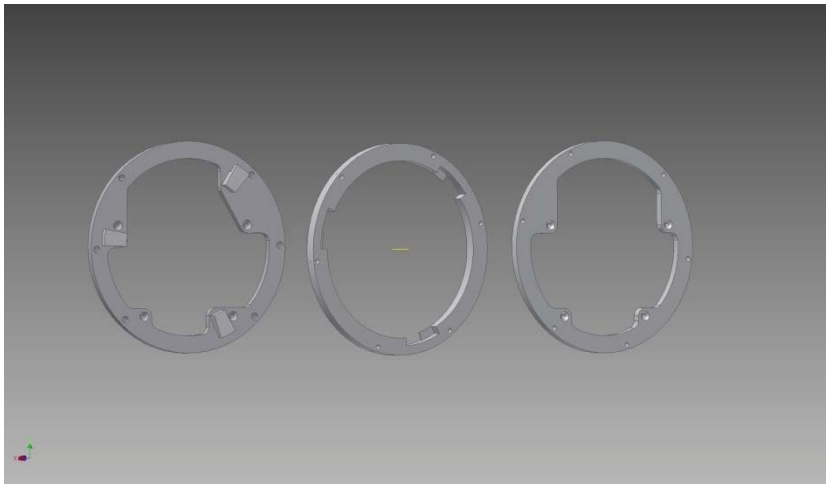

Figure 25. SPU Bulkheads. Bulkheads where used as a mounting location for all mounting plates in the SPU. They also served as a way of interlocking adjacent tubes sections. (Left) The tabs on the male bulk head interlock with the slots on the female bulkhead. (Middle) The female bulkhead mounts inside the female gland and mates with the tab on the male bulkhead. (Right) The mounting plate sits behind the female bulk head and attaches to both the upper and lower plate mounting rails.

The male and female bulkheads are named due to the fact they are mounted on the male and female interfaces of the tube sections respectively. These two bulkheads interlock to ensure adjacent tube sections remain firmly connected. The tabs on the face of the male bulkhead fit into the cutouts of the female bulkhead and then can be twisted to interlock with the female tabs. This ensures that the sub remains in one piece if the vacuum on the inner cavity breaks. The male bulkhead also contains countersunk mounting holes for the mounting rails and plates. Due to close proximity to female bulkhead's cutouts the adjacent mounting holes could not be built into the female bulkhead. As a result a secondary bulkhead was design to be mounted behind the female bulkhead and act solely as an anchor for the mounting rails.

4.5 Upper Plate Assembly

The upper plate acted as a mount for all SPU actuators. Figure 26 shows the upper plate assembly.

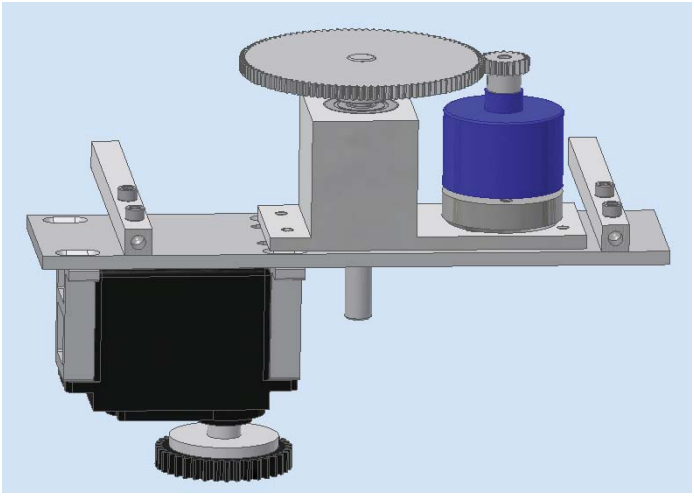

Figure 26. Final SPU Upper Plate Design. The upper plate of the SPU served as a mounting location for all actuators associated with the thruster. A gearbox and motor combination mounted on top of the plate powered the propeller. A servo mounted under the plate was used to turn the shaft and gear housing.

Servos were selected as the actuators to rotate the shaft and gear housings. A servo is a motor and gearbox combination with imbedded electronics and a potentiometer for position control. The potentiometer is a resistor that changes resistance as it rotates. Inside of the servo the motor is geared to both the output shaft and potentiometer. To control its position the circuitry receives a voltage from a servo controller which it compares with the voltage drop across the potentiometer. If the two values are unequal the motor adjusts the resistance of the potentiometer until the input voltage and the potentiometer voltage match. One down side to using a potentiometer for feedback control is that the output shaft has a finite rotational range. Servos are commercially available in a number of standard sizes with a variety of output torques, rotation angles and rotational speed. The servo can be seen mounted upside down under the plate in Figure 26. Commercially available servo mounts were used to mount the servo to the plate.

Originally it was decided to use a Hitech HS-300 servo since this model was readily available. A 38 tooth gear was mounted onto the output shaft of the servo. After bench testing it was found that this model struggled to rotate the shaft and gear housing and did not provide an

adequate range to turn the external shaft 360 degrees. Due to space constraints in the submarine the largest gear ratio that could be implemented on the servo was 1:1. The servo then would need a minimum rotational range of 360 degrees. Two possible solutions were examined for his problem. The easiest solution would be to purchase a servo capable of rotating 360 degrees. The more desirable solution however would be to remove the potentiometer and implement an external feedback system for servo positioning. This would allow the servo to spin freely in both directions and eliminate any rotational limitations on the gear and shaft housing.

The first, and simpler solution, was to replace the HS-300 servo with a more powerful servo that would better fit the needs of the SPU. After much research it was discovered that the vast majority of servos are only capable of rotations below 180^0. Select models had the option of turning continuously however an external feedback system, such as the encoder mentioned above, would need to be implemented. Only one type of servo was found to provide the rotation range required for this project. Sail winch servos are commonly used for applications for model sail boats where large rotational ranges are required. The wall of the submarine limits the size of the servo that can be mounted on the upper plate. The majority of the sail winch servos where too large to fit into the designated space in the SPU. Two possible models were found that fit both the rotational range and the size requirements for this application. The first was the VSD-10Y. This servo could turn 360^0, provide 136.04 oz-in of torque and had dimensions of 1.57x0.98x1.93inches. The second option was the Grand Wing Servo (GWS) S125 6T. This servo could complete 6 full turns, provide a torque of 142 oz-in and was smaller with dimension of 1.59x0.79x1.65 inches. Since the GWS S125 6T provided a higher rotational range and torque coupled with a smaller volume it was the primary choice for replacing the HS-300.

A concept for the second, more desirable solution was developed using an AMT 100 Series encoder driven by an auxiliary gear to measure the angular displacement of the gear and shaft housing. This type of encoder consists of a stationary outer element and a rotary internal shaft mount. The encoder is capable of measuring the speed and angular displacement of a shaft mounted in it. The encoder would provide angular feedback allowing the servo to turn continuously. Figure 27 shows two close ups of the lower plate with the encoder implemented. Figure 27b shows the encoder mounted on the underside of the bottom plate. A shaft mounted in the encoder travels through a bearing embedded in the plate to a gear on the far side which engages the directional gear on the shaft and gear housing. Figure 27a shows the gearing on the top side of the bottom plate. The bottom gear in the figure is attached to the encoder, the right gear is on the servo and the large gear in the center is attached to the shaft and gear housing. As the servo turns the housing the encoder measures the displacement of the large gear. In order for this to work the potentiometer in the servo must be removed. The SPU would then need a new controller in order to analyze the raw data from the encoder when adjusting the position.

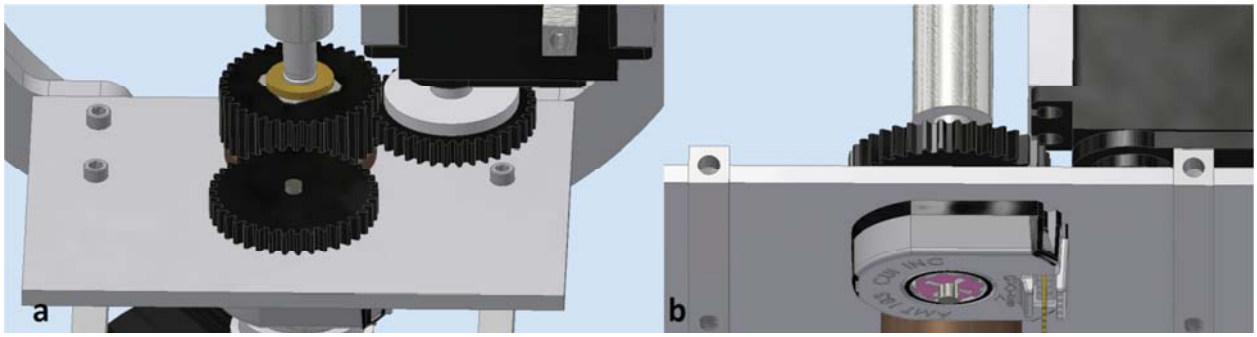

Figure 27.Servo External Encoder Feedback Concept. This concept allows the gear and shaft housing to turn continuously.(a) The gear in the foreground meshes with the large gear at the top of the shaft and gear housing transferring the motion to the encoder via a small shaft at its center.(b) The encoder mounted under the plate measures the angle and angular velocity of the shaft and provide positioning feedback to the servo.

After a more in-depth evaluation of the second, continuously turning, design, it was found that a period of no less than two weeks would be needed to design the required electronics. Since at this point neither the time nor resources needed for this undertaking were available it was decided to simply replace the current servo. Due to the high cost of the seals no PTFE seal was mounted in-between the tube section and shaft and gear housing during the initial bench testing of the servos. During the initial test the servos were capable of turning the shaft and gear housing but exhibited a strange behavior at the end of their counter clockwise rotation. When the servo would hit its mark it would reverse 5 to 10^0 clockwise keeping the servo from hitting its mark. After further testing it was found that three of the four servos obtained for use in this project exhibited this behavior. Despite this behavior the servos were next tested with the seals installed. When loaded with the combined torque from the seals and gear housing the servos struggled to turn. In order for the SPU to work properly both the resistance of the shaft and gear housing and the strange behavior of the servo would have to be compensated for.

In order to decrease the torque required from the servo, two alterations where made to the SPU design. The first was that the original graphite reinforced PTFE seals were replaced with a lower friction seal with a shallower depth rating. The second was that the 38 tooth gear mounted on the servo was replaced with a slightly smaller 32 tooth gear. The gear ratio reduced the torque required from the servo by 15.8 percent. This came at a cost of a 15.8 percent decrease in the turning range of the servo.

The second problem facing the servos was slightly more difficult to resolve. The reversing behavior the servos were exhibiting was concluded to be internal to the servo electronics. The final angle of the servo was unpredictable making the problem hard to compensate for. A GWS representative was consulted to determine if this behavior was to be expected from all S125 6T servos. The represented claimed that this behavior was due to faulty circuitry in the servo and that any future orders of GWS 125 servos would work properly. Though only one of four of the previous servos worked properly an additional order of five GWS 125 servos was placed.

Since the project deadline was approaching and it was unclear whether the GWS servos would work properly a secondary turning mechanism was designed. The initial solution was to

replace the GWS125 6T with the VSD-10Y servo discussed above. At the time however the servo was unavailable from the supplier. The only servos available with the desired range were too large to fit in the space designed to mount the servo. In order to implement one of these larger servos a secondary upper plate was designed to attach to the upper rails. This plate moved the servo mounting location toward the center of the submarine removing the size constraints due to the wall. Hitec HS785HB winch servos were purchased to be implemented with this new design. This is a much larger and stronger servo with dimensions of 2.32x1.14x1.96" and an output torque of 183.31 oz.in. Figure 28 shows the new upper shelf assembly. Due to the increase in size of the servo ¼" standoffs would need to be employed to attach the servo to the generic mounts. Though this solution would allow for a more powerful servo to be implemented in the submarine it would also require a considerable amount of machining to implement.

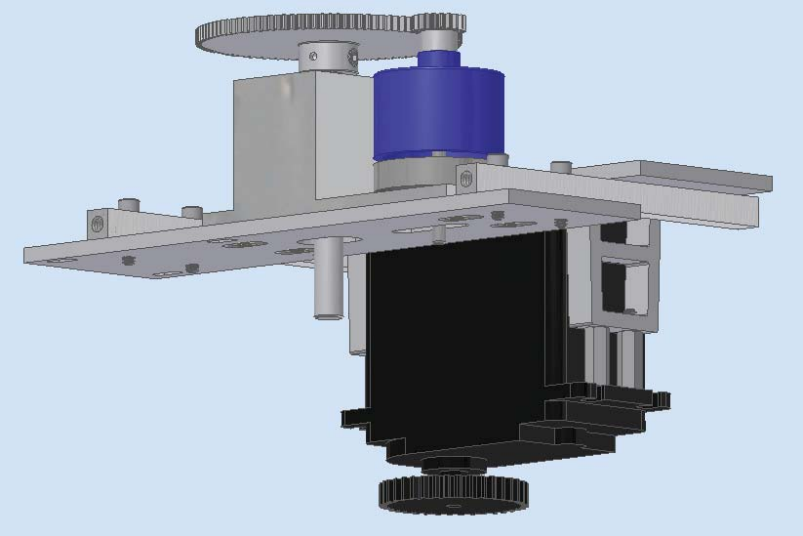

Figure 28. Large Servo Upper Platform Design. This concept was created to allow a larger servo to be implemented in the SPU. The secondary upper plate moves the servo away from the wall of the submarine greatly increasing the size of the servo that can be implemented.

Fortunately the second order of GWS servos did not exhibit the same undesirable behavior as the first and were able to be implemented effectively. Once tested with new seals and gear ratio the servos had no problem turning the shaft and gear housing.

4.6 Motor and Gearbox

A Hyperion ZS2213 brushless electric DC motor and gearbox were used to power the SPU propeller. The Hyperion motor is a newer version of the model used on the propeller test rig discussed earlier and thus was known to couple well with the setup. It contained an unloaded KV value of 862. A gearbox was designed to decrease the load on the motor and allow it to run at higher RPMs. The gearbox and motor combination can be seen in Figure 29.

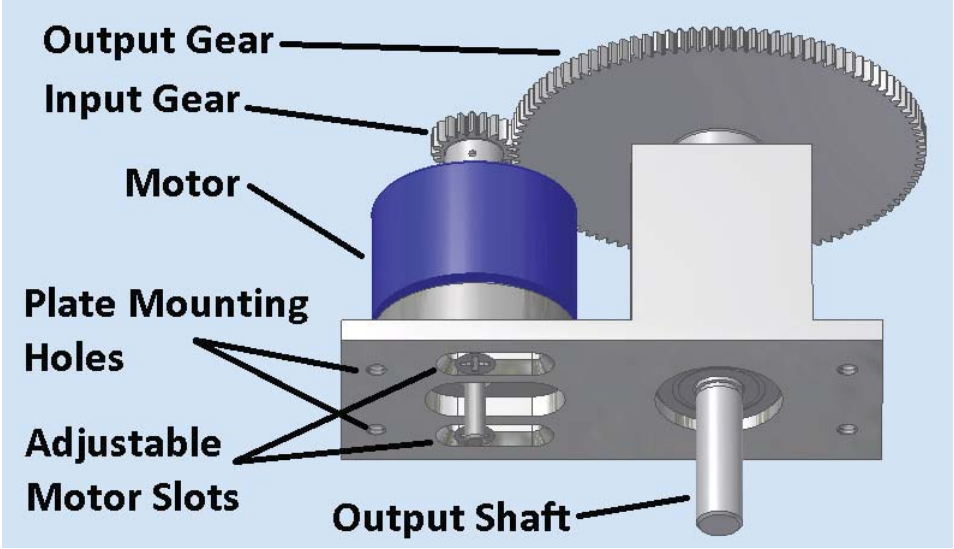

Figure 29. SPU Gearbox. This gearbox was specially designed to be implemented as the SPU propeller power source. The gear box fits most 22 cm motors and screws directly to the upper mounting plate in the SPU. The slots under the motor allow for the use of many different sizes of gears giving the gearbox an adjustable gear ratio. The current configuration has a gear ratio of 5.25.

The main body of the gearbox is machined block of aluminum. The motor mounts directly to the 1/8 inch mounting plate on the left side of the gearbox. An input gear attaches to the shaft of the motor and meshes with a larger output gear on the gear box. Slots on the mounting plate allow the motor to be adjusted so that gear meshing can occur for any shaft spacing between 1 and 1.4 inches. The output gear mounts on the output shaft that is held in place by two bearings that press fit into the aluminum block on the right side of the gearbox. The initial gearbox setup utilizes a twenty tooth input gear and a 105 tooth output gear allowing for an effective gear ratio of 5.25. This lowers the effective KV value of the motor to 164.

4.7 SPU Stability Analysis

Before the final design was approved it was essential to evaluate the stability of the submarine with the SPUs installed. The goal of this evaluation was to determine what affect the thrust from the SPU would have on the roll angle of the submarine. This could not be done without first calculating the center of buoyancy (CB) and the center of gravity (CG) for the combined vehicle. Table 1 shows all essential quantities for this calculation. The first two columns show the values and locations of the weight and buoyancy of the 690 AUV and the SPUs. These values where measured using CAD assemblies in Autodesk Inventor. The CG and CB were measured from the center of the tube section with upwards being considered the positive direction. The final column shows the values for the combined AUV. These were calculated as a weighted sum of the AUV and two SPUs. The combined vehicle weighed 103.22 lbs. and was 1.34 lbs. buoyant. The CG and CB were at -0.452 and -0.061 in. respectively.

Table 1. AUV Center of Gravity and Center of Buoyancy Values

	690 AUV	SPU	Combined
Center of Gravity (in)	-0.466	-0.339	-0.452
Center of Buoyancy (in)	-0.054	-0.122	-0.061
Weight (lbs.)	92.216	5.5	103.216
Buoyancy (lbs.)	93.159	5.7	104.559

In this evaluation the worst possible SPU configuration was considered to be when both SPUs were pointing to the port or starboard side. Figure 30 shows a free body diagram of the AUV with the black circle representing the tube sections. The dashed line represents the initial position of the SPUs lower housing before the propellers have been initiated. In this configuration the CG sits directly below CM holding the submarine in the upright position. When the propellers are initiated the additional torque on the body causes the sub to begin to list. As the list angle increases the CG moves out from under the CB which causes a restoring moment that opposes the torque due to the thruster. At some steady state angle, θ, the thruster torque and the correcting moment reach equilibrium causing the submarine to list at a constant angle. The red line in Figure 30 represents the lower housing for this scenario. It is important to minimize this steady state angle since it alters the direction of the thrust. If θ is too large it could jeopardize the dynamics of the AUV. If the torques on the body have not reached equilibrium by the time the sub has rolled 90^{o} the correcting moment begins to decrease. In this scenario the vehicle could potentially spin continuously around its CG.

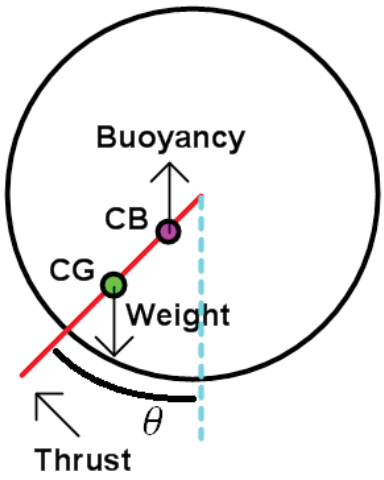

Figure 30. AUV Free-Body Diagram. This freebody diagram shows how the AUV reacts when under the power of the SPUs

For this analysis the maximum combined thrust from both SPUs was assumed to be 1.8 lbs. An equation for θ was derived by summing the moments on the body around the CG. Since θ is a steady state value this summation must equal zero. Solving this equation for θ produces Equation 7. In this equation F_T is the SPU thrust, D_T is the initial vertical distance (when F_T is zero) to the propeller hub from the CG and F_B is the buoyancy of the submarine.

$$\theta = \sin^{-1} \frac{F_T * D_T}{F_B(CB - CG)} \tag{7}$$

Evaluating this equation predicted a worst case list of 21°. Though this would induce a minor vertical component to the thrust it was considered an acceptable steady state angle. It is important to note that this is a static evaluation. As the body begins to move hydrodynamic forces affect the dynamics of the submarine. Since the SPUs are designed to operate at low velocities these forces were assumed to be negligible.

4.8 Manufacturing and Assembly

The assembly of the two SPUs required a total 36 machined parts. The manufacturing of the parts was divided between two machine shops. All parts requiring anodizing where handled by Redco. A machine shop based in Bedford, Virginia. All other parts were manufactured by Metal Processing Inc. based in Radford, Virginia. Manufacturing took approximately eight weeks due to complications machining the lower housing. Once all parts had been received the thrusters were assembled in house. Assembly and adjustments took an additional two weeks. Figure 31 shows the completed SPUs. The left SPU is positioned male end up and the right SPU shows the view through the female gland.

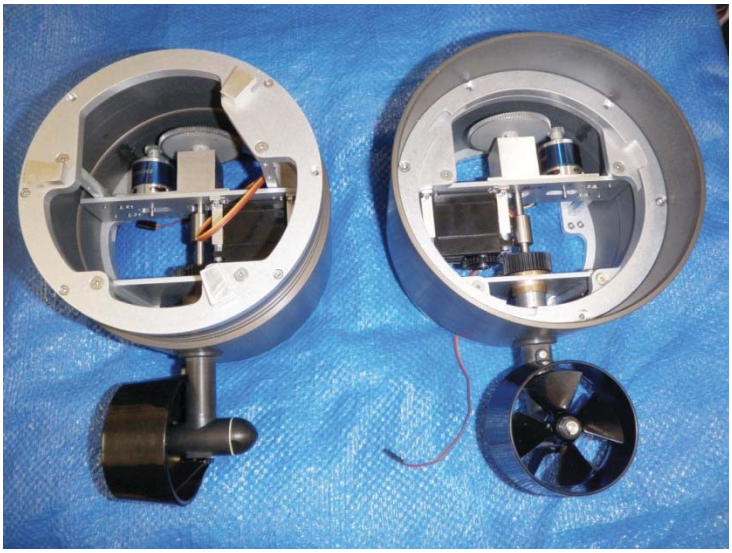

Figure 31. Final SPU Assemblies. This figure shows both completley assembled SPUs. The SPU on the left is positioned with the male gland up and the right SPU provides a look through the female gland.

4.9 SPU Integration

The majority of the work done integrating the SPU into the AUV was completed by the Electrical and Computer Engineering members of the Autonomous Systems and Controls Lab at

Virginia Tech. This work included adapting the control software to run on the 690 computer system and adjusting internal circuitry to be compatible with the SPUs. Once adapted to the AUV a vacuum was pulled on the inner cavity to ensure that all seals where working effectively. Once the vacuum had held for 72 hours initial bench testing was performed to test the behavior of the SPUs.

For bench testing a simulator was implemented on the computer of the 690 AUV. This program was used to simulate a marine environment that the sub was tasked with navigating. As the submarine actuated the SPUs and its control surfaces the simulator would calculate the theoretical changes in heading and velocity and feed it back to the submarine. During these simulations the SPUs were found to be quite noisy due to the gearing in the lower housing. Though this was not desirable this was not a design constraint placed on the SPUs. When actuated by the code the GWS servos had a tendency to slightly undershoot their marks. This was thought to be a combination of the resistance of the lower gear housing and low resolution of the potentiometer imbedded in the servo. External servo feedback could be implemented to reduce the undershooting of the servos but, as previously discussed, was not feasible at this time. The fully assembled 690 AUV with integrated SPUs can be seen in Figure 32. In this figure the SPUs are facing to the port side of the vehicle.

Figure 32. Virginia Tech 690 AUV with Integrated SPU Thrusters. The SPU tube sections can be seen aft of the submarine head and forward of the tail section. The lower housings and ducted propellers suspend below the body of the sub.

4.10 SPU Pool Testing

Finalized testing of the SPUs was completed in the dive well of War Memorial Pool located on the campus of Virginia Tech. Testing was conducted by programing the submarine to follow a straight path across the surface of the pool. The initial orientation of the sub was 40° off the desired path. The sub had to navigate back to the path and follow it until testing was complete. Figure 33 shows the results of the maneuver tests. The red line shows the desired path and the blue line shows the actual path of the vehicle. Tests with disabled SPUs are shown in the left figures and test with SPUs enabled are shown in the right figures. All measurements were taken in SI units due to the software used. Tests were run at 0.5, 1 and 2 m/s which correspond to 1.64, 3.28 and 6.56 ft/s. The figures at the top show the 0.5 m/s cases, the middle are the 1 m/s cases and the bottom are the 2m/s case. The axes on the graphs have been varied for each speed to best show the effects of the SPUs.

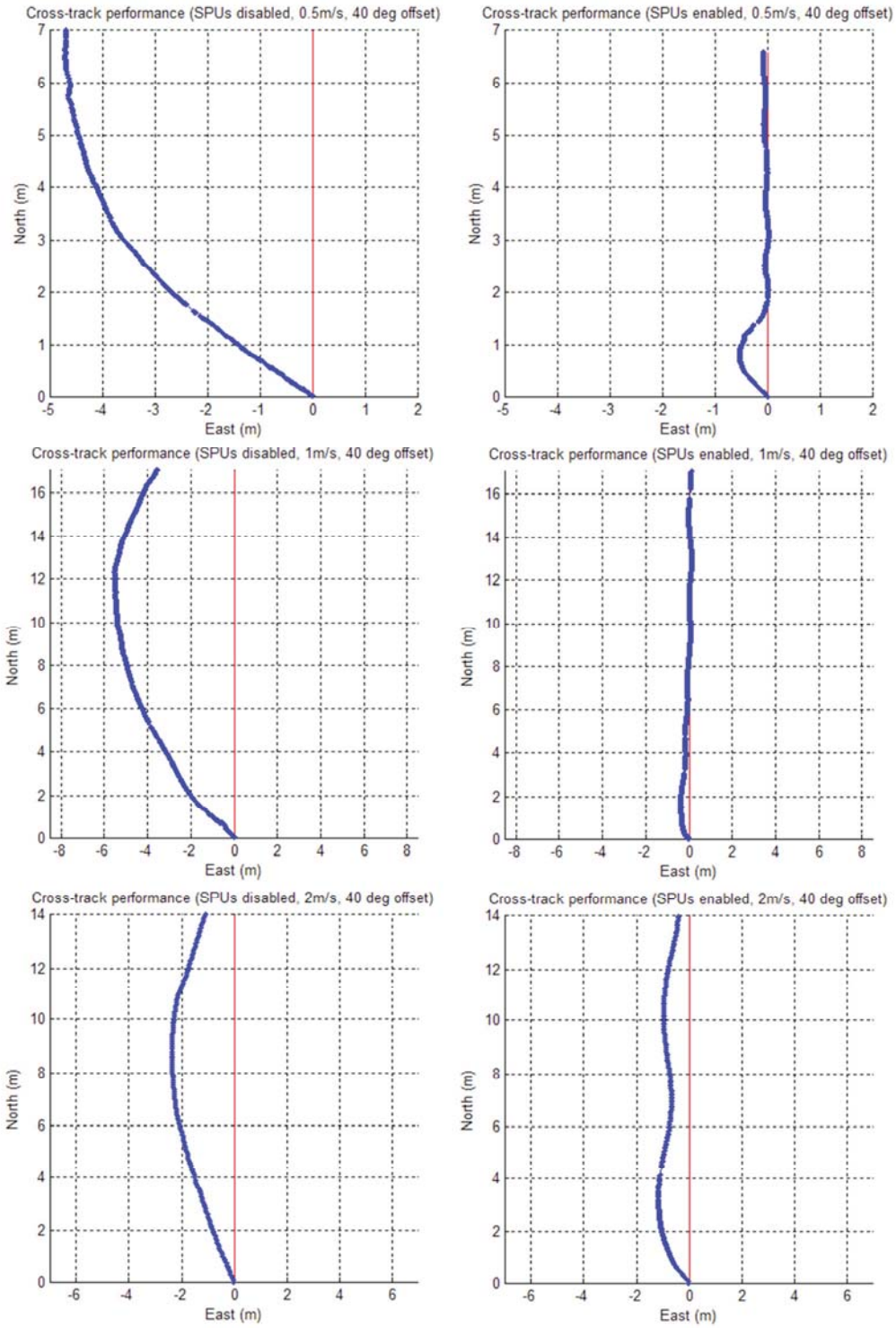

Figure 33. Virginia Tech 690 AUV SPU Maneuvering Test Results. The graphs above show the paths the 690 AUV followed during maneuver testing. The red line shows the desired path and the blue line shows the actual path the AUV followed. The graphs on the left show the performance using the control surfaces and the graphs on the right show the performance with the SPU enabled. Tests were conducted at speeds of 0.5, 1 and 2 m/s. These results are shown from top to bottom respectively.

At the lower velocities the SPUs made a significant difference in the maneuverability of the sub. In the 0.5 m/s case with the SPUs enabled the sub traveled half a meter off course before turning and maneuvering back to the designated path. At approximately 2 meters along the designated path the sub was successfully tracking the line. At the same speed with the SPUs disabled the sub traveled almost 5 meters off course and had not turned back to the designated line at 7 meters down the path. The 1 m/s cases produced results comparable to the 0.5 m/s cases. This behavior was to be expected since the forces on the control surfaces are proportional to the speed of the vehicle.

The SPUs were found to be slightly less effective in the 2 m/s cases. At these higher speeds the forces on the control surfaces are much larger allowing for better control of the vehicle. With the SPUs enabled the vehicle stayed well within 2 meters of the desired path. With disabled SPUs the vehicle strayed over 2 meters from the path. In both cases the vehicle failed to reconnect with the path after 14 meters. This performance was acceptable since the main purpose of the SPUs was to maneuver the vehicle in low velocity scenarios such as the 0.5 and 1 m/s case.

Chapter 5: Conclusions

Overall the finalized SPU fulfilled the requirements set fourth at the beginning of the project. Though many research hours were spent investigating a concept that ultimately failed, this is often the case in a design based research project. In the end, the geared rim driven design was shown to be inefficient but the rim driven design as a whole was a feasible concept. A rim driven thruster was found being advertised by a company in the UK. This design is implemented in many modern day exploratory AUVs. From a thruster standpoint this motorized rim driven design could have more than satisfied the thruster requirements. However, in a design based project all design constraints must be considered. In this case time and funds prevented implementation of the motorized rim driven design. Though the rim driven concept was set aside the research done to evaluate its performance ultimately presented the next feasible design.

The non-retractable azimuthing thruster that was studied as a benchmarking tool while designing rim driven propellers was the next design considered. The thruster was used as inspiration to design a housing that would extend below a modular tube section. A series of gears and shafts powered a ducted propeller mounted to the bottom of the housing. The housing itself was capable of rotating independently of the tube section allowing the propeller to direct thrust in the horizontal plane. Standard size PTFE seals were implemented in the housing to cut down on design costs. These seals were rated to allow the housing and tube section to operate in depths over 300 ft.

Inside the tube sections a series of bulkheads and mounting plates were used to hold electronics and actuators required by the SPU. The primary power source of the propeller was a Hyperion ZS2213 brushless electric DC motor coupled with a gearbox with an adjustable gear ratio. The gearbox was mounted on the upper plate directly above lower housing. The output shaft of the gearbox was connected to primary drive shaft with a standard 1/4 inch coupler. A GWS S125 6T servo was geared to the top of the lower housing to allow for azimuthing capabilities.

The final testing of the SPUs showed a considerable increase in maneuverability in low speed scenarios. At a velocity of 0.5 m/s and an off set of 40^{o} from a designate path the sub was able to reconnect with the path after 2 meters. Without the SPUs the sub failed to reconnect with the path and strayed off course almost 5 meters. During the high speed test however the SPU became less effective. This was considered acceptable since the main function of the SPUs was to increase maneuverability in low speed scenarios. Overall the SPUs were found to be a highly effective way of increasing low speed maneuverability of the AUV.

Bibliography

[1] Briggs, Robert. "Mechanical Design of a Self-Mooring Autonomous Underwater Vehicle." MA thesis. Masters of Science in Aerospace Engineering, 2012. Print.

[2] Neu, Wayne. *AOE 3264 Resistance and Propulsion of Ships: Propulsion*. Print.

[3] Lewis, Edward. *Principles of Naval Architecture: Volume II: Resistance, Propulsion and Vibration*. Jersey City, NJ: The Society of Naval Architects and Marine Engineers, 1988. 135-145. Print.

[4] Duelley, Richard. "Autonomous Underwater Vehicle Propulsion Design." MS thesis. Masters of Science in Aerospace Engineering, 2012. Print.

[5] SchottelantriebII. Retrieved November 20,2012, from http://www.graupner.de/de/products/2335/product.aspx

[6] IntegratedThruster™. Retrieved November 20,2012 from http://www.tsltechnology.com/marine/thrusters.htm

[7] SAIL WINCH S125 SERIES. Retrieved November 20,2012, from http://www.gwsus.com/english/product/servo/s125.htm

[8] VSD-10Y 360 Degree Servo 12kg. Retrieved on November 20,2012 from: www.hobbyking.com